Luminescence in $p-i-n$ structures with compensated quantum wells

© R.B. Adamov[1], G.A. Melentev[1], A.A. Podoskin[2], M.I. Kondratov[2], A.E. Grishin[2], S.O. Slipchenko[2], I.V. Sedova[2], S.V. Sorokin[2], G.V. Klimko[2], I.S. Makhov[3], D.A. Firsov[1], V.A. Shalygin[1,¶]

[1] Peter the Great St. Petersburg Polytechnic University,
195251 St. Petersburg, Russia
[2] Ioffe Institute,
194021 St. Petersburg, Russia
[3] HSE University,
190008 St. Petersburg, Russia
¶ E-mail: shalygin@rphf.spbstu.ru

Received November 14, 2023
Revised November 26, 2023
Accepted November 29, 2023

Photo- and electroluminescence in $p-i-n$ structures with compensated GaAs/AlGaAs quantum wells have been studied. Two structures with different doping profiles were studied: with spatial separation of donors and acceptors (donors are localized in quantum wells, while acceptors are localized in barriers) and without it (both donors and acceptors are localized in quantum wells). The studies were carried out in the near-IR range at helium temperatures. Luminescence lines due to electron transitions from donor states to the first heavy-hole subband ($D-hh1$) and from the first electron subband to acceptor states ($e1-A$) have been identified. At large electric currents, the near-IR lasing due to these transitions was observed in the electroluminescence spectra. It has been found that the integrated lasing intensity related to the $D-hh1$ transitions in the structure without a spatial separation of donors and acceptors was three times higher than in the structure with the spatial separation. It is these transitions that ensure effective depletion of donor levels, which is important for the donor-assisted terahertz emission at $e1-D$ electron transitions. The results of the work can be used in the development of electrically pumped terahertz emitters.

Keywords: quantum wells, $p-i-n$ structures, GaAs, AlAs, photoluminescence, electroluminescence, near-infrared range.

DOI: 10.61011/SC.2023.08.57620.5748

1. Introduction

Terahertz (THz) radiation is increasingly used in science and technology (see [1,2] and references therein). Solid-state THz radiation sources with electrical pumping are especially convenient for practical applications. First of all, these are quantum cascade lasers (QCL), based on intersubband transitions in quantum wells (QW). One of the recent achievements is a QCL with a radiation frequency of 4 THz, operating up to a temperature of 261 K [3,4]. However, the widespread use of quantum cascade lasers is limited by the high cost of such devices, due to the extremely complex technology of their production. A potential alternative is THz radiation emitters that use impurity transitions of charge carriers in bulk semiconductors and nanostructures. This mechanism of THz radiation emission can be realized by injection of non-equilibrium charge carriers in the $p-n$ junction. Experimental studies of injection emitters of terahertz radiation based on impurity transitions in bulk semiconductors were carried out in $p-n$ structures based on 4H-SiC [5] and silicon [6]. There was also THz electroluminescence (EL) in δ-doped p-GaAs/AlAs quantum wells placed between two p^+-GaAs layers [7].

Recently, THz photoluminescence (PL) in nanostructures with compensated GaAs/AlGaAs quantum wells was discovered and studied [8–10]. It was shown that the main contributions to THz PL are due to electron transitions from the first size-quantization subband in the conduction band ($e1$) and excited states of donors ($D2p_{xy}$) to the ground donor level ($D1s$). It has been established that a noticeable gain in the integral intensity of THz emission under optical pumping is provided by structures with spatial separation of donors and acceptors (when donors are localized in quantum wells, and acceptors — in barriers) compared to structures in which both donors and acceptors were localized in quantum wells. The reason is that the spatial separation of donors and acceptors turns off the undesirable competing mechanism of recombination of non-equilibrium electrons of the subband $e1$ with holes at the ground level of acceptors ($A1s$) [10].

It seems promising to use compensated GaAs/AlGaAs quantum wells to create electrically pumped THz emitters. For example, one can grow an $p-i-n$ structure on a conducting n-GaAs substrate by placing an n-AlGaAs:Si emitter between the substrate and an active layer with compensated quantum wells (i-layer) followed by growing an p-AlGaAs:Be emitter. When such diode structures are directly biased, the injection of electrons from the n-emitter and holes from the p-emitter into the i-layer will occur, followed by the capture of nonequilibrium charge carriers into quantum wells. As a result, it can be expected that under these conditions, radiative processes similar to those observed in compensated quantum wells under optical pumping will be observed [9,10]. Transitions of

non-equilibrium electrons $e1-D1s$ will be accompanied by the radiation emission in THz photons, and recombination transitions $D1s-hh1$, accompanied by emission of the near-infrared (NIR) range, will ensure effective depletion of donor levels $D1s$.

In this work, we study NIR luminescence in $p-i-n$ structures with compensated GaAs/AlGaAs quantum wells at a temperature of 10 K. There was a study of a structure with spatial separation of donors and acceptors, as well as a structure in which both donors and acceptors were localized in quantum wells. The studies were carried out under both optical and electrical pumping. The main channels of radiative recombination were determined under various experimental conditions. In addition, the current-voltage characteristics (CVC) of $p-i-n$ diodes made from these structures were studied. The main goal of the work is to compare the prospects for using the two studied structures with compensated quantum wells to create THz radiation emitters with electrical pumping.

2. Samples

Heterostructures with selectively doped multiple quantum wells (MQW) were grown by molecular-beam epitaxy on silicon-doped n^+-GaAs (001) „epi-ready“ substrates using a two-chamber SemiTEq setup (Russia). The substrate was doped with silicon, the doping level was $(2-3)\cdot 10^{18}\,\mathrm{cm}^{-3}$. Standard gallium and aluminum effusion cells, as well as a valved arsenic cracker cell (Veeco, USA) were used as sources of molecular beams. Silicon and beryllium were used as n- and p-type dopants, respectively. The substrate temperature during growth of the entire structure was 580°C.

Two heterostructures were grown (hereinafter denoted by the letters W and B). Each of them included the following layers (in the direction from the substrate to the surface): a buffer layer n-GaAs with a thickness of ~ 500 nm (with an electron concentration of $n\sim 10^{18}\,\mathrm{cm}^{-3}$), an n-emitter $Al_{0.9}Ga_{0.1}As$:Si with a thickness of $1\,\mu$m ($n\sim 10^{18}\,\mathrm{cm}^{-3}$), undoped waveguide layer $Al_{0.3}Ga_{0.7}As$ with 50 GaAs quantum wells (width $L_{QW}=7.7$ nm), separated by barriers $Al_{0.3}Ga_{0.7}As$ (width 7.3 nm), undoped waveguide layer $Al_{0.3}Ga_{0.7}As$ 0.1 μm thick, p-emitter $Al_{0.9}Ga_{0.1}As$:Be 1 μm thick (with hole concentration $p\sim 5\cdot 10^{17}\,\mathrm{cm}^{-3}$) and contact layer p^{++}-GaAs 0.4 μm thick ($p\sim 10^{19}\,\mathrm{cm}^{-3}$). The parameters of the grown structures with MQW (their period and width of quantum wells) were determined using X-ray diffractometry (XRD analysis) and photoluminescence spectra in the NIR range.

The W and B heterostructures had different doping schemes for quantum wells and barriers. In one case (structure W), the central part (~ 2.6 nm) of GaAs quantum wells was doped simultaneously with both donors and acceptors with approximately the same concentration $\sim 1.2\cdot 10^{17}\,\mathrm{cm}^{-3}$ (which corresponds to the surface concentration of Si and Be $\sim 3\cdot 10^{10}\,\mathrm{cm}^{-2}$), while the barriers remained undoped. In another case (structure B, see Figure 1), the central part (~ 2.6 nm) of GaAs quantum wells was doped only with donors (the volume and surface concentrations of Si atoms were $\sim 1.2\cdot 10^{17}\,\mathrm{cm}^{-3}$ and $\sim 3\cdot 10^{10}\,\mathrm{cm}^{-2}$, respectively), and the barriers were doped with acceptors only. The central part (~ 5 nm) of each barrier was doped, and the surface concentration of Be atoms was also ensured at the level of $\sim 3\cdot 10^{10}\,\mathrm{cm}^{-2}$ (the volume concentration of Be atoms was $\sim 0.6\cdot 10^{17}\,\mathrm{cm}^{-3}$). To balance the concentrations of donors and acceptors near the external GaAs quantum wells, the near-boundary regions of both waveguide layers (2.5 nm thick at a distance of ~ 1.0 nm from the AlGaAs/GaAs interface) were doped with Be with a bulk concentration of $\sim 0.6\cdot 10^{17}\,\mathrm{cm}^{-3}$.

To study luminescence, rectangular samples were prepared from both structures by cleaving along cleavage planes. Photoluminescence studies were carried out on samples with lateral dimensions 4×4 mm. For electroluminescence studies, separate two-terminal devices with lateral dimensions 0.5×2 mm were manufactured. To pass an electric current, multilayer metal contacts were used: an Au-Ge/Au contact was deposited on the back side of the n^+-GaAs substrate, and a Ti/Pt/Au contact was created on top of the p^{++}-GaAs layer. Each device made on the basis of an W or B heterostructure is an $p-i-n$ diode, since multiple quantum wells have the intrinsic conductivity due to compensation of donors by acceptors. The diodes were soldered p-side to the copper heat sinks using indium solder.

3. Photoluminescence Studies

The samples under study were mounted on the cold finger of a Janis closed-cycle optical cryostat PTCM-4–7. Optical pumping of the samples was carried out using a continuous solid-state laser at a wavelength of 532 nm. The laser beam was focused at the center of the sample surface into a spot with a diameter of 510 μm. The beam power varied within 0.1–100 mW. The PL radiation was collected through a fused silica window in the direction normal to the emitting surface at a solid angle of 0.12 sr. PL spectra in the NIR range were studied using a Horiba Jobin Yvon FHR-640 monochromator equipped with a holographic diffraction grating (1200 lines/mm) and a silicon CCD matrix. The studies were carried out in the photon energy range 1450–1600 meV with a spectral resolution ~ 0.1 meV.

PL spectra from the surface of the B and W structures at a temperature of 10 K are presented in Figure 2. When the photon energy $\hbar\omega$ is less than the band gap of gallium arsenide $E_g(\mathrm{GaAs})=1519$ meV, the PL spectra of both structures coincide within the measurement error. There is a broad luminescence band with a maximum intensity at $\hbar\omega\cong 1480$ meV, and the spectral shape of this band does not depend on pumping, and the integral intensity varies linearly with the photoexcitation power. Obviously, this PL

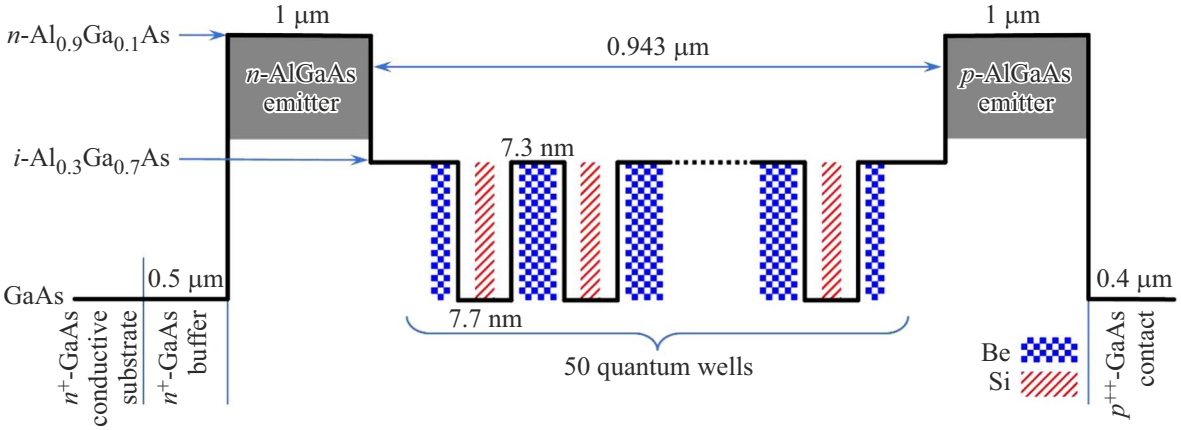

Figure 1. Schematic diagram of the $p-i-n$ structure with doped QW with spatial separation of donors and acceptors (structure B). The thick line shows the potential profile of the conduction band bottom.

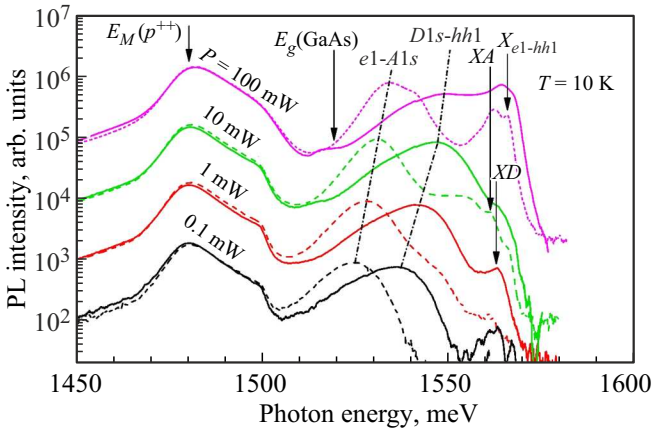

Figure 2. Photoluminescence spectra from the surface of structures B (solid lines) and W (dashed lines) at different optical pumping powers. The dash-dotted lines demonstrate a shift of the PL line maxima due to the $D1s-hh1$ ($e1-A1s$) transitions with increasing pumping power for the B (W) structure. The arrows indicate the spectral positions of the exciton recombination line maxima for QWs (XA, XD and X_{e1-hh1}) and characteristic energies for the p^{++}-GaAs layer in the studied structures. (The colored version of the figure is available on-line).

band is formed by the upper contact layer p^{++}-GaAs, whose parameters were the same for the structures B and W. The features of NIR PL of heavily doped gallium arsenide were studied in detail in works [11–13]. It was shown that at hole concentrations $\sim 10^{19}\,\mathrm{cm}^{-3}$, the acceptor impurity band merges with the valence band. Radiative recombination of non-equilibrium holes in this band with electrons in the conduction band can be described as a combination of direct and indirect interband transitions. At low temperatures, the shape of the interband recombination line has a stepped shoulder on the high-frequency side, the spectral position of which is determined by the Fermi level. The spectral positions of this shoulder and the maximum point of the spectral line are unambiguously related to the hole concentration. In the PL spectra we obtained, these are 1499 meV and $E_M(p^{++}) = 1480$ meV, respectively. According to the data of the work [11], these parameters correspond to p-GaAs with a hole concentration $\sim 10^{19}\,\mathrm{cm}^{-3}$, which coincides with the hole concentration in the contact layer p^{++}-GaAs for the studied structures B and W.

At photon energies $\hbar\omega > E_g$(GaAs), the PL spectra are caused by processes in quantum wells. For the structures B and W the spectra are significantly different (see Figure 2). The spectra can reveal the same spontaneous PL lines that were previously identified in similar structures with compensated quantum wells without n- and p-emitters [9]. Thus, in the structure B at pumping powers 0.1–10 mW, the $D1s-hh1$ line dominates, caused by electron transitions from the ground levels of donors to the first subband of heavy holes. With an increase in pumping by 2 orders of magnitude, the maximum intensity of this line undergoes a blue shift from 1537 meV by +10 meV, and the magnitude of the shift is proportional to $\ln(P/P_m)$, where (P/P_m) is pumping power P, normalized to the minimum pumping power $P_m = 0.1$ mW. Let us note that the line width (measured at its half-maximum) remains virtually unchanged (20–21 meV). This shift may be due to two reasons. The first is due to the fact that the donor-doped layer in the QW has a non-zero width (it amounts to $\sim 30\%$ of the well width). As is known, the binding energy is maximum for donors localized in the center of the well and decreases as the donors move away from the center. At low pump levels, recombination from the deepest donor levels, which are populated by non-equilibrium electrons first, predominates. With increasing pumping, these transitions gradually become saturated and transitions from shallow levels become more and more intense, which leads to „a blue“ shift of the resulting PL line at $D1s-hh1$ transitions. At sufficiently high concentrations of non-equilibrium holes in the $hh1$ subband, this mechanism comes to naught, but another one gradually turns on. It is due to the fact that the quasi-Fermi level

for holes shifts deeper into the $hh1$ subband as pumping increases.

In the spectral region $\hbar\omega > E_g(\text{GaAs})$ under weak pumping, there is also a weak narrow peak at $\hbar\omega = 1562.6$ meV, which corresponds to the recombination of an exciton bound to the donor (XD) [9]. When pumped at 100 mW, the excitonic line XD becomes dominant.

The PL spectra of the W structure are dominated by the asymmetric line $e1{-}A1s$, caused by the recombination of free electrons in the $e1$ subband with holes at the ground acceptor level [9]. With an increase in pump power by 3 orders of magnitude, this line demonstrates „a blue shift" from 1525 meV by +9 meV (see Figure 2) and a decrease in width from 16 to 13 meV, while its maximum intensity increases in proportion to the pumping level. The „blue" shift of this line as pumping increases is caused by the finite width of the acceptor-doped layer in QW (and the dependence of the acceptor binding energy on its location in the well), as well as a shift of the quasi-Fermi level for electrons up the subband $e1$.

In addition, at maximum pumping, two excitonic lines are also visible in the PL spectrum of the structure W. The line at $\hbar\omega = 1561$ meV is due to the recombination of the exciton bound to the acceptor (XA), and the photon energy of 1565.6 meV corresponds to the radiative recombination of free excitons (X_{e1-hh1}), formed from electrons of the subband $e1$ and holes of the subband $hh1$. The arguments for identifying NIR PL lines in compensated quantum wells are presented in more detail in the work [9].

As noted above, the spectral positions of the maxima of the $D1s{-}hh1$ line (in the B structure) and the $e1{-}A1s$ line (in the W structure) change monotonically with the intensity of optical pumping. This allows to estimate how much in the structures studied here the pump radiation is attenuated in the contact layer p^{++}-GaAs and in the p-emitter before it reaches the active layer with quantum wells. Thus, in the structure B at a pumping power of 10 mW (intensity 4.9 W/cm^2) there is a maximum of the $D1s{-}hh1$ line at $\hbar\omega = 1546.7$ meV. The same position of the maximum of this line for a similar structure without an p-emitter and an p^{++}-GaAs contact layer corresponds to a pump intensity of 1.5 W/cm^2 (see [9]). Thus, the pump radiation intensity is attenuated by the upper conducting layers of the B structure by a factor of 3.2. In a similar way, based on the dependence of the spectral position of the maximum of the $e1{-}A1s$ line in the W structure on the pumping intensity, the optical losses in the conducting layers of this structure were determined: the laser pumping radiation is attenuated by a factor of 6.3. For convenience, we introduce the quantity I_i, which characterizes the effective intensity of optical pumping of the active layer of the B and W structures, taking into account optical losses in the contact layer p^{++}-GaAs and p-emitter.

Since electroluminescence was subsequently studied in the same structures, and the design of the samples provided the possibility of detecting EL radiation from the ends of the structures and did not allow studying radiation from the surface, photoluminescence from the ends of the structures B and W was additionally studied (photoexcitation in this case is still carried out in the center of the square front surface of the structure). An analysis of the PL emission spectra collected from the end of the structure showed that the $D1s{-}hh1$ line (in the QW of the B structure) and the $e1{-}A1s$ line (in the QW of the W structure), as well as the line of interband recombination radiation in the contact layer p^{++}-GaAs have the same patterns that were identified in the spectra of PL emission collected directly from the excited surface. The PL spectra from the end are fundamentally different in that they lack excitonic recombination lines. This is due to the self-absorption effect: the recombination radiation of excitons excited in the center of the structure is almost completely absorbed on the path from the generation region to the end of the structure due to the large absorption coefficient in the exciton resonance region ($> 10^3$ cm^{-1} [14]).

4. Electroluminescence Studies

For electroluminescence studies, the same spectral setup was used as for photoluminescence studies. $P{-}i{-}n$ diodes made from B and W structures (see Section 2) were mounted on the cold finger of the cryostat using a copper holder. EL radiation was collected from the narrow end of the diodes (0.5 mm). The studies were carried out with forward bias. At weak injection currents, measurements were carried out at direct current until the power dissipated in the diode reached 60 mW, while the Joule heating of the diode was negligible. A Keithley 2601A voltage and current source-meter was used for these experiments. Measurements at higher currents were carried out in a pulsed mode using periodic pulses with a duration of 1 μs with a repetition rate of 87 Hz. In this case, the time-averaged power dissipation did not exceed 10 mW. To generate current pulses, a generator of an original design was used. Oscillograms of current and voltage pulses were recorded using a Tektronix TDS2024B oscilloscope. The measurement regions in direct current and pulsed mode overlapped in the range of currents 5–50 mA, where both measurement methods gave identical results — up to the measurement error. The use of two measurement methods made it possible to cover a wide range of excitation levels: the magnitude of the injection current varied within 4 orders of magnitude. Let us note that the flow of electric current through the p^{++}-GaAs contact layer does not lead to interband luminescence in this layer, since, unlike the case of interband photoexcitation, it is not accompanied by the generation of non-equilibrium electrons and holes. Therefore, the EL spectra were recorded at photon energies $\hbar\omega > E_g(\text{GaAs})$.

Electroluminescence spectra for an $p{-}i{-}n$ diode made from the B structure are presented in Figure 3. At injection currents 0.16–78 mA, there is one broad line of ~ 21 meV width in the EL spectrum, which experiences a „blue" shift

with increasing current. Comparing this line with the PL spectra of the B structure (Figure 2), we can conclude that this line is caused by spontaneous emission at $D1s-hh1$ transitions. The spectral position of the maximum of the $D1s-hh1$ line in the EL spectrum at a current of 0.16 A (1544.6 meV) coincides with the spectral position of this line in the PL spectrum (see Figure 2) at an optical pumping power of 3.2 mW (which corresponds to the effective intensity of the pumping beam $I_i = 0.49\,\mathrm{W/cm^2}$). Based on this, to a first approximation, we can conclude that the indicated injection current and optical pumping power provide the same levels of excitation of non-equilibrium charge carriers in quantum wells.

The magnitude of the „blue" shift of this line in the case of EL is somewhat lower compared to PL. When the pump level changes by 2 orders of magnitude, the $D1s-hh1$ line in the EL spectra shifts by +7.5 meV (see Figure 3), and in the PL spectra by +10 meV. The decrease in the „blue" shift rate under conditions of electric current flow is explained by the action of the electric field, which leads to the quantum-size Stark effect. This will be discussed in more detail later.

When the injection current increases from 78 to 180 mA, the $D1s-hh1$ line experiences a sharp „red" shift by 7 meV, and with a further increase in the current to 1.5 A, there is an additional „red" displacement, but the speed of this displacement noticeably decreases. At currents of 1.7 A or more, intense narrow peaks appear on the low-frequency wing of the spontaneous EL line, apparently associated with laser generation.

The „red" shift becomes clear when analyzing the current-voltage characteristics of the B diode (see Figure 4). At voltages < 5.8 V, an exponential increase in current with voltage is observed, which is characteristic of light-emitting diodes based on GaAs/AlGaAs heterostructures [15,16]. The CVC then demonstrates a region of negative differential conductance (NDC). In this section, the current decreases slightly ($< 20\%$), and the voltage increases sharply from 5.8 to 9.3 V. Under these conditions, there were current instabilities: oscillations in the current and voltage oscillograms. With a further increase in voltage, the current initially increases exponentially with voltage, and then, when the resistance of the active layer becomes less than the resistance of the outer layers of the structure (the latter, according to our estimate, has a value of ~ 0.4 Ohm), the current-voltage curve tends to reach a linear dependence. Let us note that the NDC region was previously experimentally observed in work [17] at helium temperature in n^+-n-n^+ structures with $GaAs/Al_{0.36}Ga_{0.64}As$ quantum wells with a width of 7 nm. In the work, it was shown that the features of the current-voltage characteristics of such a structure under forward bias are explained by the effects of resonant tunneling that arise under the sequential formation of high-field domains in quantum wells. In the structures we are studying, the active layer has parameters close to the parameters of the active layer in the work [17], and the width of the NDC section for the B diode is 3.5 V, which

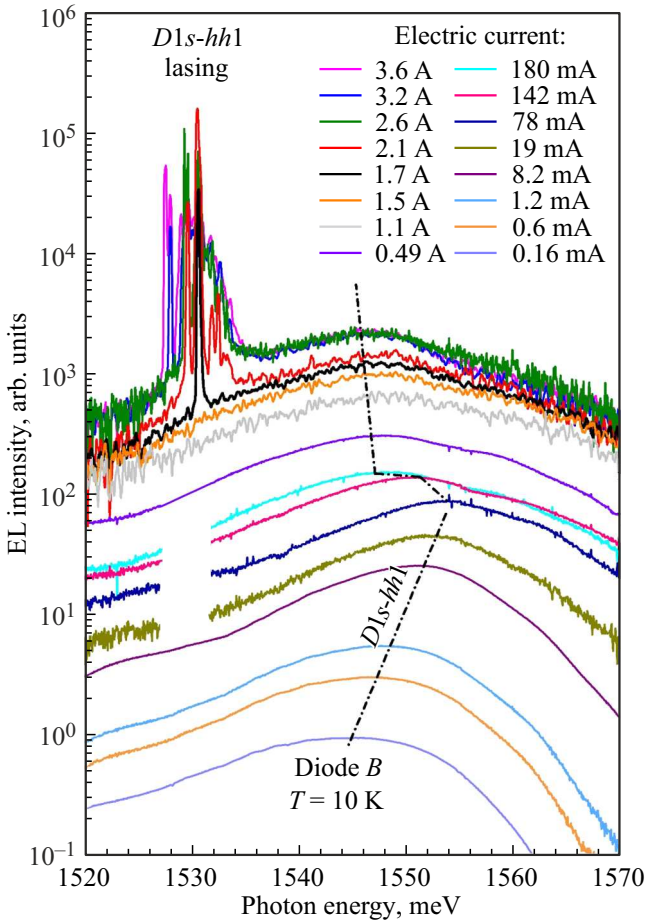

Figure 3. Electroluminescence spectra at different injection currents for an $p-i-n$ diode made from the B structure. The dash-dot line shows the positions of the maxima of the spontaneous emission band caused by the $D1s-hh1$ transitions. Sharp peaks at high currents demonstrate lasing due to these transitions. Measurements at currents 0.16–8.2 mA were carried out in DC regime and measurements at higher currents were performed in pulsed mode (The colored version of the figure is available online).

is close to the width of the NDC section on the current-voltage curve in the cited work (~ 3.2 B), therefore we also associate the observed current instabilities with resonant tunneling.

Note that the section of the sharp „red" shift of the spontaneous EL line in Figure 3 begins at a current through the diode of 78 mA and ends at a current of 180 mA. On the CVC, the first of these points precedes the beginning of the NDC section, and the second corresponds to its end. If we calculate the electric field strength F_i in the active layer of the structure, taking into account ohmic losses in its outer layers, it turns out that at the beginning of the NDC section it amounts to $\sim 6 \cdot 10^4$ V/cm, and at the end is 10^5 V/cm. This suggests that the observed „red" shift of the $D1s-hh1$ line by ~ 7 meV is due to the Stark effect. This hypothesis is confirmed by

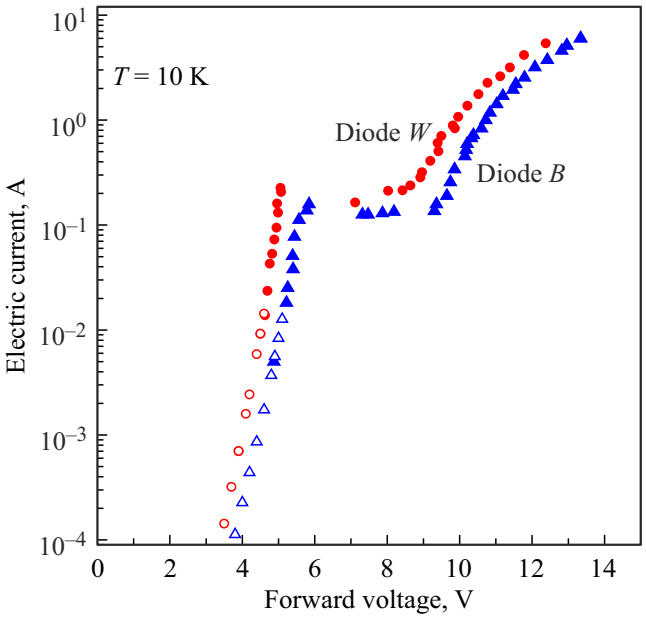

Figure 4. Current-voltage characteristics of $p-i-n$ diodes made from structures B and W. Lateral dimensions of samples: 0.5×2 mm. DC measurements are shown with empty symbols. The results of measurements using voltage pulses with a duration of 1 μs are presented with filled symbols.

calculations of the quantum-size Stark effect, published in the work [18], according to which, when the electric field increases from $6 \cdot 10^4$ to 10^5 V/cm in $Al_{0.3}Ga_{0.7}As$ quantum wells of 10 nm width, the size-quantization level for electrons E_1 drops down by 4 meV, and valence level HH_1 rises up by 9 meV. Our quantum wells have a smaller width (7.7 nm). Since the magnitudes of the Stark shifts ΔE_1 and ΔHH_1 are proportional, respectively, to $(eF_iL_{QW})^2/E_1$ and $(eF_iL_{QW})^2/HH_1$ [18], the Stark shifts for the diode B under study will be smaller: $\Delta E_1 \approx -1.5$ meV and $\Delta HH_1 \approx +4$ meV. Due to this, the energy of the radiative transition $D1s-hh1$ when passing through the NDC band should change by $\Delta E_1 - \Delta HH_1 \approx -6$ meV, which is close to the value of the „red“ shift of the $D1s-hh1$ (~ 7 meV) observed in the experiment.

The behavior of the spontaneous EL line $D1s-hh1$ is demonstrated in more detail in Figure 5, *a*. At pump currents $J = 0.1-1$ mA, this line experiences a „blue“ shift, the magnitude of which is proportional to $\ln(J/J_0)$, which is similar to the above dependence $\ln(P/P_0)$ for the „blue“ shift in luminescence spectra under optical pumping. However, with an increase in the injection current up to 78 mA, the value of the blue shift of the EL line $D1s-hh1$ begins to lag behind the $\ln(J/J_0)$ dependence, which can be largely associated with the superposition of the „red“ shift due to the Stark effect. In the NDC region, the injection current and, consequently, the concentrations of nonequilibrium charge carriers in the QW practically do not change, and the Stark effect manifests itself in its pure form, leading, as discussed above, to a sharp „red“ shift. At bias voltages exceeding the upper limit of the NDC region, which corresponds to pump currents from 180 mA to 3.6 A, the spontaneous EL line $D1s-hh1$ demonstrates a „red shift“, but it is relatively small (~ 1.5 meV). The latter circumstance is due to the fact that when the injection current changes by an order of magnitude, the „blue“ shift discussed above noticeably increases, which is superimposed on the „red“ Stark shift and reduces its resulting value.

Figure 5, *a* also shows the current dependence of the intensity at the maximum of the spontaneous emission line caused by the $D1s-hh1$ transitions for the diode B. This dependence is linear at weak pumping (which is also typical for luminescence under optical pumping) and becomes sublinear when the quantum-size Stark effect begins to manifest itself. The dependence again becomes linear in

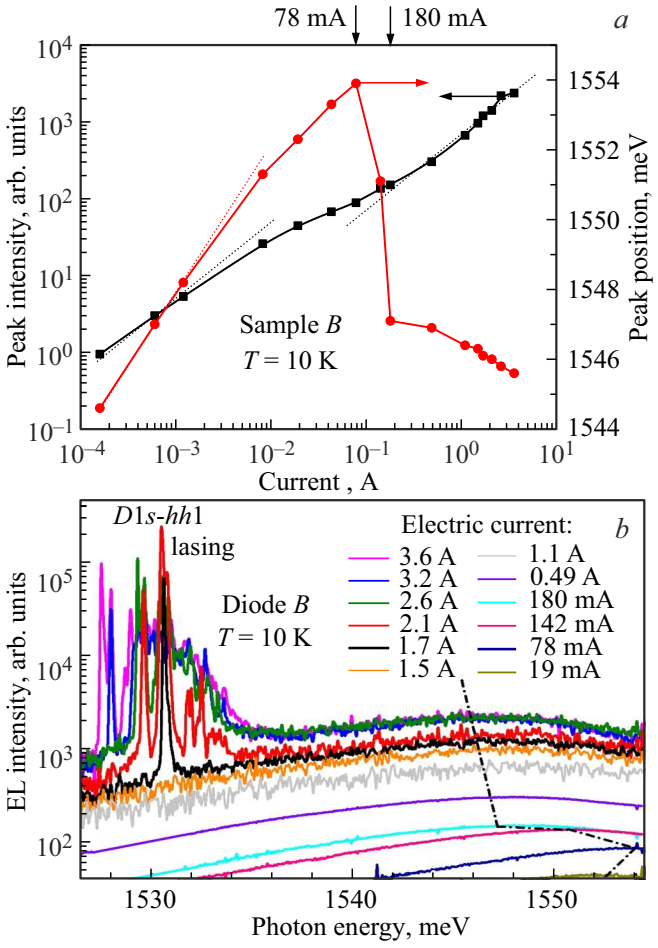

Figure 5. *a* — the position of the maximum (right axis) and the intensity at the maximum (left axis) of the line of spontaneous emission caused by the $D1s-hh1$ transitions, depending on the electric current in the diode B. Straight dotted lines show linear sections of dependencies. Solid lines are a guide for the eye. *b* — mode structure of stimulated emission of the diode B. The dash-dot line shows the positions of the maxima of the spontaneous emission band caused by the $D1s-hh1$ transitions. (The colored version of the figure is available on-line).

the range of currents beyond the upper boundary of the NDC region, when the „blue“ shift and the Stark shift of the spontaneous EL line $D1s-hh1$ almost compensate each other.

Let us move on to a discussion of the process of stimulated radiation emission, which was in the diode B at pumping currents of 1.7 A or more. Since the diodes under study were manufactured by cleaving grown GaAs/AlGaAs structures along cleavage planes, the ends of the diode were two pairs of ideally plane-parallel mirrors with mutually orthogonal arrangement of planes. In such structures, high-Q closed modes of stimulated emission can arise due to the effect of total internal reflection [19,20]. Figure 5, *b* allows to trace how the mode structure of stimulated emission changes depending on the injection current in the diode. At the lasing threshold ($J \approx 1.7$ A), there is a single line with a photon energy of 1530.60 meV and a width of 0.09 meV, which coincides with the spectral resolution of the experimental setup. Thus, the quality factor of this line itself, determined through the ratio of the lasing wavelength to the true line width at half maximum (after subtracting hardware broadening), significantly exceeds $2 \cdot 10^4$. The laser line appears on the low-frequency wing of the spontaneous EL line $D1s-hh1$ (the maximum of the spontaneous EL line is at a photon energy of 1545.6 meV) and is obviously caused by precisely these transitions. As the current through the diode increases, additional closed modes arise, characterized by a different number of reflections from the cleaved edges. At currents of 2.6 A and more, individual lines of closed modes merge into stimulated emission bands several meV wide.

The transformation of the EL spectra of the W diode with varying injection current has a more complex character (see Figures 6 and 7). Let us first note that the W diode, in which both donors and compensating acceptors are localized in a narrow layer at the center of the QW, provides large injection currents over the entire range of forward biases compared to the B diode, in which the donors and acceptors are spatially separated (see CVC in Figure 4). In the first case, there are no space charges in the active layer of the structure, and in the second there are regions with a positive space charge of ionized donors at the center of the quantum wells, as well as regions with a negative space charge of ionized acceptors over 2/3 of the barrier thickness. According to the calculation, the built-in field strength in the region free of space charges is ~ 2300 V/cm. This field, which penetrates each QW/barrier interface (it is directed from the QW to the barrier), prevents the tunneling of injected electrons through the barriers separating the QW and promotes the tunneling of injected holes. Obviously, the contribution of injected electrons to the total current through the diode exceeds the contribution of injected holes, so the weakening of the first contribution due to the built-in field leads to a decrease in the total current in the B diode compared to the W diode (for a given forward bias).

When studying PL in similar structures without emitters, it was found that in a structure of the W type under

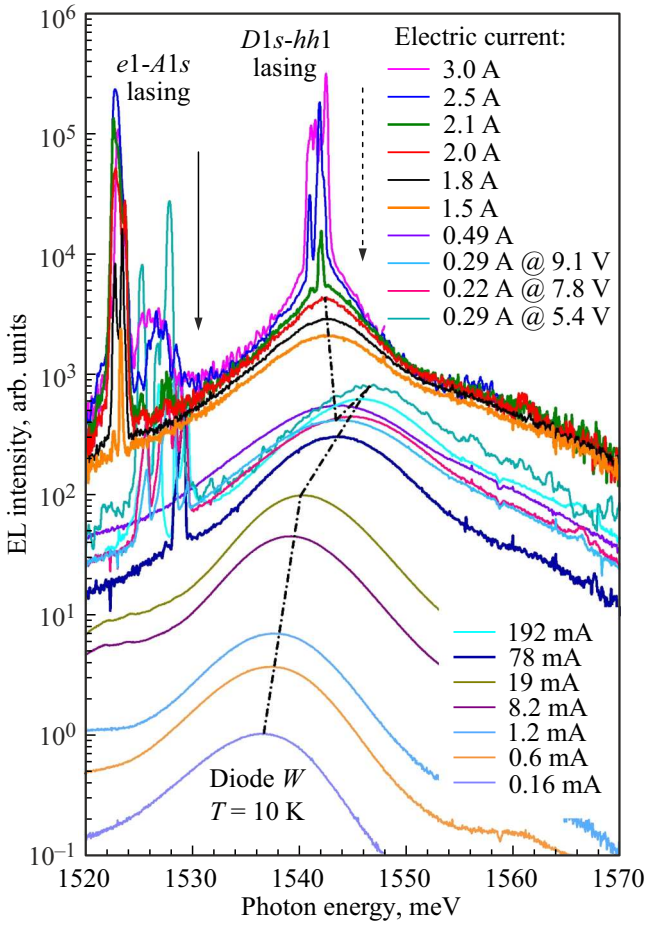

Figure 6. Electroluminescence spectra at different injection currents for an $p-i-n$ diode made on the basis of the W structure. The dash-dot line shows the spectral position of the maxima of the spontaneous emission band. A series of narrow peaks at high currents are associated with lasing at the $e1-A1$ and $D1s-hh1$ transitions. The solid and dashed arrows indicate, respectively, the positions of the laser line and the maximum of the spontaneous EL line for the $D1s-hh1$ transitions in the B diode at the lasing threshold. (The colored version of the figure is available on-line).

weak pumping (< 1 W/cm^2), the amplitude of the $e1-A1s$ line is an order of magnitude greater than that of the $D1s-hh1$ line. As the pumping level increases, both lines monotonically increase their amplitude, but the relative contribution of the $e1-A1s$ line to the integral intensity of spontaneous emission increases more slowly compared to the $D1s-hh1$ line. As a result, when ~ 9 W/cm^2 is pumped, the amplitudes of these lines in the PL spectrum become equal, and since their relative spectral shift is small (~ 7 meV, i.e., ~ 2 times smaller than the width of the lines themselves), they merge together, while the resulting line of spontaneous luminescence has a maximum at a point midway between the spectral positions of the maxima of the two lines (1533.5 meV). For > 20 W/cm^2 pumping, the dominant contribution to the resulting spontaneous luminescence line is made by $D1s-hh1$ transitions. With an increase in the intensity of optical pumping by approxi-

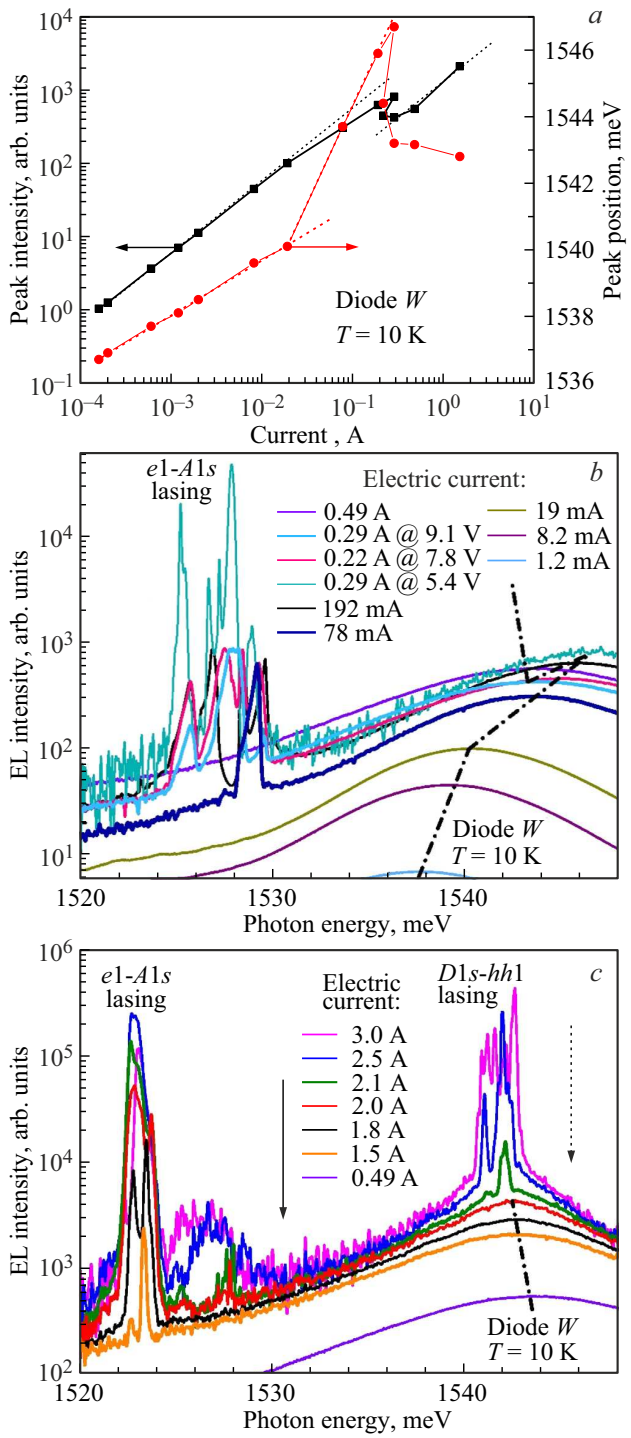

Figure 7. *a* — the position of the maximum (right axis) and the intensity at the maximum (left axis) of the band of spontaneous emission, depending on the electric current in the diode *W*. Straight dotted lines show linear sections of dependencies. Solid lines are a guide for the eye. *b, c* — mode structure of stimulated emission of the diode *W* at different injection currents. The dash-dot line shows the spectral position of the maxima of the spontaneous emission band. The solid and dashed arrows indicate, respectively, the positions of the laser line and the maximum of the spontaneous EL line for the $D1s-hh1$ transitions in the *B* diode at the lasing threshold. (The colored version of the figure is available on-line).

mately one order of magnitude (from 1 to 20 W/cm^2), when in spontaneous PL the dominance of the $e1-A1s$ transitions is replaced by the dominance of the $D1s-hh1$ transitions, the maximum of the resulting spontaneous PL line at the $e1-A1s$ and $D1s-hh1$ transitions experiences quite large „blue“ shift: ~ 8 meV.

In the *W* structure studied here, the upper layers attenuate optical pumping by a factor of ~ 6, however, at a maximum pumping of 100 mW (which corresponds to the effective intensity of photoexcitation of the active layer with quantum wells $I_i \approx 8$ W/cm^2), the appearance of a protrusion on the high-frequency wing of the $e1-A1s$ line is noticeable in the PL spectrum. caused by the overlap of the $D1s-hh1$ line with the $e1-A1s$ line (see Figure 2). We do not present experimental PL spectra at higher pumping levels, since their interpretation is difficult due to heating of the samples.

Let us proceed on to the analysis of the EL spectra of the structure *W* (Figures 6 and 7). At a minimum injection current of 0.16 mA, there is a maximum of the spontaneous EL line at the photon energy ~ 1537 meV. It can be argued that in this case, the level of excitation of non-equilibrium electrons and holes in quantum wells significantly exceeds the level achieved at the effective intensity of optical excitation of the active layer of the structure *B* $I_i \approx 8$ W/cm^2. Indeed, according to the PL spectra of this structure (Figure 2), observation of the spontaneous PL line of the structure *W* at such a photon energy requires an optical pump power > 100 mW, and therefore an effective intensity > 8 W/cm^2. As noted above, at such excitation levels, the spontaneous PL line in this structure contains contributions from both $e1-A1s$ and $D1s-hh1$ transitions, with the latter being dominant.

Note that at a minimum injection current $J = 0.16$ mA, the excitation level of nonequilibrium electrons and holes in the diode *W* exceeds the excitation level in the structure *B* by more than an order of magnitude. Therefore, it is not surprising that the current threshold for laser lasing in the *W* diode (on $e1-A1s$ transitions) turned out to be 22 times lower than in the *B* diode (on $D1s-hh1$ transitions). At $J \approx 78$ mA, a single laser line appears on the low-frequency wing of the spontaneous EL line $e1-A1s$. Unlike the *B* diode, in the *W* diode the lasing threshold precedes the NDC section on the CVC, which begins at a bias of 5.4 V and a current of 290 mA (see Figure 4). Throughout the entire section of the NDC, new closed modes of stimulated emission arise and at the same time there is a sharp „red“ shift in the spontaneous emission line, which we associate with the quantum-size Stark effect (see Figures 6 and 7, *a*). Beyond the NDC section, as the current increases, the maximum of the spontaneous emission line continues to experience a „red“ shift, only at a lower speed, and laser generation is interrupted (at a current ~ 0.49 A). Apparently, the disruption of generation is associated with an increase in optical absorption in the active layer of the structure under the transformation of the energy spectrum of electrons due to the quantum-size Stark effect [20].

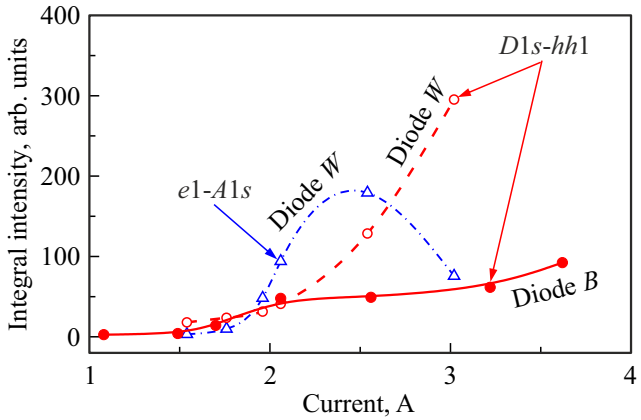

Figure 8. Integral intensity of stimulated emission of diodes B and W at different injection currents. Filled (empty) circles correspond to emission due to $D1s-hh1$ transitions in the B diode (W diode). The triangles demonstrate the lasing intensity at the $e1-A1s$ transitions in the W diode. Curves are a guide for the eye.

A further increase in the current again leads to the generation of various closed modes at the $e1-A1s$ transitions (see spectra in Figures 6 and 7, b at $J = 1.5-2$ A). In this case, a single line at the lasing threshold is shifted by -6 meV relative to the laser line at a current $J \approx 78$ mA, which is also associated with the quantum-size Stark effect.

With an even stronger injection ($J \approx 2.1$ A), a single laser line appears with a photon energy of 1542.03 meV. We believe that this line is due to the $D1s-hh1$ transitions. This is supported by the fact that in the diode B at a close current value we observed the appearance of the first lasing mode at a photon energy of 1530.60 meV on the low-frequency wing of the spontaneous EL line $D1s-hh1$ with a maximum at 1545.6 meV (these energies are indicated in Figures 6 and 7, a with solid and dashed arrows, respectively). The laser line at 1542.03 meV also lies on the low-frequency wing of this spontaneous EL line.

The current dependence of the intensity at the maximum of the spontaneous emission band for the diode W has a more complex form than for the diode B (see Figures 5, a and 7, a). It becomes non-monotonic in the NDC region, when the electric field sharply increases and a restructuring of the electron energy spectrum occurs. The observed N-pattern of this dependence for the W diode is apparently associated with the redistribution of recombination fluxes of free electrons and holes between the $e1-A1s/A1s-hh1$ and $e1-D1s/D1s-hh1$ channels.

It is interesting to compare the integral intensities of stimulated emission at the $D1s-hh1$ transitions for the diodes B and W, since these transitions are relevant for developing terahertz emitters based on $e1-D1s$ transitions. The integrated intensity was calculated in a band that covers the entire range of closed modes at $D1s-hh1$ transitions: $\hbar\omega = 1526-1536$ meV for diode B and $\hbar\omega = 1537-1547$ meV for diode W. The current dependences of the integral intensities under lasing condition are presented in Figure 8. The figure also shows the current dependence of the integral intensity of stimulated emission at $e1-A1s$ transitions for the W diode (calculation was carried out in the $\hbar\omega = 1520-1530$ meV band). It can be concluded that in the W diode, under conditions of simultaneous lasing on the $e1-A1s$ and $D1s-hh1$ transitions at currents > 2.5 A, a redistribution of recombination fluxes of free electrons and holes occurs between the $e1-A1s/A1s-hh1$ and $e1-D1s/D1s-hh1$ channels in favor of the latter. Meanwhile, the W diode can provide a fivefold gain in the intensity of the $D1s-hh1$ radiative transitions compared to the B diode. This means that compensated quantum wells under simultaneous doping with donors and acceptors at the center of quantum wells are more preferable for developing THz emitters one$1-D1s$ transitions compared to the case of spatial separation of donors and acceptors. It should be noted that this result was unexpected, since in studies of NIR photoluminescence in similar structures with compensated quantum wells the result was exactly the opposite [10].

5. Conclusion

The work carried out studies of luminescence in the near-infrared range in $p-i-n$ structures with compensated GaAs/AlGaAs quantum wells. Structures with different distribution profiles of donor (Si) and acceptor (Be) impurities were studied. Luminescence under interband optical pumping was studied directly on grown structures. Diodes with lateral dimensions 0.5×2 mm were manufactured for electroluminescence studies. All experiments were carried out at helium temperature.

The photoluminescence spectra reveal lines of radiative recombination of nonequilibrium electrons and holes in quantum wells associated with the participation of impurity levels: electron transitions from the ground states of donors $D1s$ to the first heavy-hole subband $hh1$ and transitions from the first electron subband $e1$ to the ground levels of acceptors $A1s$. In addition, peaks caused by free and bound excitons in quantum wells, as well as a wide band of interband luminescence in the surface contact layer of p^{++}-GaAs, were detected. The resulting spectra were used to interpret electroluminescence spectra.

When forward biasing $p-i-n$ diodes, the current-voltage characteristics and electroluminescence spectra were studied. In the CVC, there were areas with negative differential conductivity, due to the formation of high-field domains in quantum wells and resonantr tunneling. The electroluminescence spectra with increasing injection current in the diode first demonstrate a „blue“ shift of the recombination lines associated with the impurity levels $D1s$ and $A1s$, which is also observed in the photoluminescence spectra with increasing pumping and is associated with an increase in the concentrations of non-equilibrium electrons and holes in quantum wells. At higher injection currents, in the region of negative differential conductivity, there is

a „red“ shift of these electroluminescence lines, caused by the quantum-size Stark effect. At certain excitation levels, stimulated emission at the $D1s-hh1$ and /or $e1-A1s$ transitions is observed in the electroluminescence spectra, associated with the excitation of high-Q closed modes due to the effect of total internal reflection on the four cleaved edges of the diode.

It has been established that a structure with compensated quantum wells under simultaneous doping with donors and acceptors at the center of the quantum wells provides a fivefold gain in the integral intensity of stimulated emission at $D1s-hh1$ transitions compared to a structure with spatial separation of donors and acceptors (when donors are localized in quantum wells, and acceptors are localized in barriers). $D1s-hh1$ transitions are relevant for developing THz radiation sources, since they provide dynamic depletion of the $D1s$ levels, which are the final states for $e1-D1s$ radiative transitions corresponding to the THz range.

Thus, the spatial separation of donors and acceptors in the MQW layers of $p-i-n$ structures is impractical. To develope sources of terahertz radiation with electrical pumping, structures with selective doping of quantum wells simultaneously with both donors and acceptors are more promising.

Funding

The work of the authors R.B. Adamov, G.A. Melentyev and V.A. Shalygin was supported by the Russian Science Foundation (grant No. 22-22-00103).

Acknowledgments

The authors would like to thank M.V. Maksimov for discussing the design of $p-i-n$ structures with quantum wells.

Conflict of interest

The authors declare that they have no conflict of interest.

References

[1] M. Tonouchi. Nature Photonics, **1** (2), 97 (2007). https://doi.org/10.1038/nphoton.2007.3
[2] D.M. Mittleman. J. Appl. Phys., **122** (23), 230901 (2017). https://doi.org/10.1063/1.5007683
[3] A. Khalatpour, A.K. Paulsen, C. Deimert, Z.R. Wasilewski, Q. Hu. Nature Photonics, **15** (1), 16 (2021). https://doi.org/10.1038/s41566-020-00707-5
[4] A. Khalatpour, M.C. Tam, S.J. Addamane, J. Reno, Z. Wasilewski, Q. Hu. Appl. Phys. Lett., **122** (16), 161101 (2023). https://doi.org/10.1063/5.0144705
[5] A.V. Andrianov, J.P. Gupta, J. Kolodzey, V.I. Sankin, A.O. Zakhar'in, Yu.B. Vasil'ev. Appl. Phys. Lett., **103** (22), 221101 (2013). https://doi.org/10.1063/1.4832824
[6] A.O. Zakhar'in, Y.B. Vasilyev, N.A. Sobolev, V.V. Zabrodskii, S.V. Egorov, A.V. Andrianov. Semiconductors, **51** (5), 604 (2017) http://dx.doi.org/10.21883/FTP.2017.05.44420.8432
[7] S.M. Li, W.M. Zheng, A.L. Wu, W.Y. Cong, J. Liu, N.N. Chu, Y.X. Song. Appl. Phys. Lett., **97** (2), 023507 (2010). https://doi.org/10.1063/1.3463467
[8] I.S. Makhov, V.Yu. Panevin, D.A. Firsov, L.E. Vorobjev, G.V. Klimko. J. Appl. Phys., **126** (17), 175702 (2019). https://doi.org/10.1063/1.5121835
[9] R.B. Adamov, A.D. Petruk, G.A. Melentev, I.V. Sedova, S.V. Sorokin, I.S. Makhov, D.A. Firsov, V.A. Shalygin. St. Petersburg State Polytechnical University Journal: Physics and Mathematics., **15** (4), 32 (2022). https://doi.org/10.18721/JPM.15402
[10] R.B. Adamov, G.A. Melentev, I.V. Sedova, S.V. Sorokin, G.V. Klimko, I.S. Makhov, D.A. Firsov, V.A. Shalygin. J. Luminesc., **266**, 120302 (2024). https://doi.org/10.1016/j.jlumin.2023.120302
[11] D. Olego, M. Cardona. Phys. Rev. B, **22** (2), 886 (1980). https://doi.org/10.1103/PhysRevB.22.886
[12] M.S. Feng, C.S. Ares Fang, H.D. Chen. Mater. Chem. Phys., **42** (2), 143 (1995). https://doi.org/10.1016/0254-0584(95)01566-3
[13] S.V. Poltavtsev, R.I. Dzhioev, V.L. Korenev, I.A. Akimov, D. Kudlacik, D.R. Yakovlev, M. Bayer. Phys. Rev. B, **102** (1), 014204 (2020). https://doi.org/10.1103/PhysRevB.102.014204
[14] G. Bastard. *Wave Mechanics Applied to Semiconductor Heterostructures* (Les Ulis, Les Editions de Physique, 1988).
[15] A.E. Zhukov, N.Y. Gordeev, Y.M. Shernyakov, A.S. Payusov, A.A. Serin, M.M. Kulagina, S.A. Mintairov, N.A. Kalyuzhnyi, M.V. Maksimov. Technical Physics Letters, **44** (8), 675 (2018). http://dx.doi.org/10.21883/PJTF.2018.15.46439.17345
[16] A.V. Malevskaya, N.A. Kalyuzhnyy, F.Y. Soldatenkov, R.V. Levin, R.A. Salii, D.A. Malevskii, P.V. Pokrovskii, V.R. Larionov, V.M. Andreev. Technical Physics, **68** (1), 161 (2023). http://dx.doi.org/10.21883/JTF.2023.01.54078.166-22
[17] K.-K. Choi, B.F. Levine, C.G. Bethea, J. Walker, R.J. Malik. Appl. Phys. Lett., **50** (25), 1814 (1987). https://doi.org/10.1063/1.97706
[18] G. Bastard, J.A. Brum, R. Ferreira. Solid State Phys., **44**, 229 (1991). https://doi.org/10.1016/S0081-1947(08)60092-2
[19] A.A. Podoskin, D.N. Romanovich, I.S. Shashkin, P.S. Gavrina, Z.N. Sokolova, S.O. Slipchenko, N.A. Pikhtin. Semiconductors, **53** (6), 828 (2019). http://dx.doi.org/10.21883/FTP.2019.06.47739.9058a
[20] A.A. Podoskin, D.N. Romanovich, I.S. Shashkin, P.S. Gavrina, Z.N. Sokolova, S.O. Slipchenko, N.A. Pikhtin. Semiconductors, **54** (5), 581 (2020). http://dx.doi.org/10.21883/FTP.2020.05.49266.9343

Translated by EgoTranslating